Characterization of a shallow-bound 0_g^+ valence state of I_2 using emission from the D $0_u^+(^3P_2)$ and F′ $0_u^+(^1D_2)$ ion-pair states populated by amplified spontaneous emission

Trevor Ridley,*[a] Kenneth P. Lawley,[a] Robert J. Donovan[a] and Vadim A. Alekseev[b]

Received 17th July 2007, Accepted 17th September 2007
First published as an Advance Article on the web 26th September 2007
DOI: 10.1039/b710924e

A range of vibrational levels of the D $0_u^+(^3P_2)$ and F′ $0_u^+(^1D_2)$ ion-pair states of I_2 is shown to be easily generated by amplified spontaneous emission (ASE) from their more accessible partners, E $0_g^+(^3P_2)$ and f′ $0_g^+(^1D_2)$, in sufficient concentration for dispersed fluorescence studies of the D $0_u^+(^3P_2) \rightarrow 0_g^+$(bb) and F′ $0_u^+(^1D_2) \rightarrow 0_g^+$(bb) transitions to be carried out. T_0 ($J = 49$) of this shallow-bound 0_g^+(bb) valence state is unambiguously determined and an improved R_e value of 3.952 ± 0.005 Å is obtained from optimizing the fit of the intensities of the vibrational progressions in the 0_g^+(bb) state, and T_e is found to be 27311.3 ± 2 cm^{-1}, leading to $D_e = 442.0 \pm 2$ cm^{-1}.

1. Introduction

Excitation of high-lying electronic states of atoms and molecules using laser radiation frequently creates favourable conditions for the macroscopic radiative effect known as amplified spontaneous emission (ASE). If the concentration of excited states reaches a critical level, ASE transfers a significant fraction of the upper state population to a lower state by a dipole-allowed transition in a time that is short compared to the radiative lifetime. The threshold concentration, N_c, for the ASE effect is given[1] by

$$N_c = N_i - N_k = 8\pi\Delta\nu/L\lambda^2 A_{ik}, \quad (1)$$

where $N_{i(k)}$ is the population of the upper (lower) level, L is the length of the active medium, and $\Delta\nu$, λ and A_{ik} are the spectral width, wavelength and Einstein coefficient, respectively. In most cases the spectral width is due to the Doppler effect, $\Delta\nu \sim \lambda^{-1}$ and, since $A_{ik} \sim \lambda^{-3}\langle v_i|v_k\rangle^2\mu_{ik}(R)^2$, where $\langle v_i|v_k\rangle^2$ is the Franck–Condon (FC) factor and $\mu_{ik}(R)$ is the electronic transition dipole, eqn (1) may be reduced to

$$N_c = \text{const}/L\langle v_i|v_k\rangle^2\mu_{ik}(R)^2 \quad (2)$$

i.e. the threshold concentration is wavelength independent, but the ASE process may be triggered in a way that is wavelength dependent, *e.g.* by black-body radiation in the far infra-red, by spontaneous emission or by photons in the wings of any exciting laser radiation.

In a recent letter[2] we presented evidence for infra-red ASE between two pairs of ion-pair states of the I_2 molecule, namely E $0_g^+(^3P_2)$/D $0_u^+(^3P_2)$ and γ $1_u(^3P_2)$/β $1_g(^3P_2)$. The E $0_g^+(^3P_2)$ ($v = 0$) and D $0_u^+(^3P_2)$ ($v = 0$) levels are separated by only 388 cm^{-1}, and the γ $1_u(^3P_2)$/β $1_g(^3P_2)$ pair by 795 cm^{-1}. It appears that, if the critical concentration can be achieved, ASE provides an efficient way of changing the g/u parity of ion-pair states in a homonuclear halogen molecule. This is particularly useful if the vibrational levels to which the ASE transfer occurs cannot be efficiently accessed by more conventional pathways. In the present paper, we describe the use of this phenomenon to characterize the 0_g^+(bb) state of I_2, a weakly-bound valence state that correlates with the third dissociation limit, I*($^2P_{1/2}$) + I*($^2P_{1/2}$), designated (bb). The range of vibrational levels to which ASE transfer can take place is determined by the FC factors for the rovibronic transition[2] rather than an energy-matching criterion, *e.g.* ASE transfer from ($v = 0$) of the E $0_g^+(^3P_2)$ goes almost uniquely to ($v = 0$) of the D $0_u^+(^3P_2)$ state.

In a previous paper[3] we observed fluorescence to the 0_g^+(bb) state from the F′ $0_u^+(^1D_2)$ ion-pair state that was excited by two different excitation pathways, both of which were very inefficient. Consequently, it was not possible to resolve the vibrational structure in the dispersed emission spectra. However, it was shown that the spectra were consistent with being due to emission to a state that is bound by $\sim$450 cm^{-1}, as predicted by *ab initio* calculations.[4] In the present paper, we show that vibrationally-resolved spectra are readily observed when using ASE to populate the D $0_u^+(^3P_2)$ and F′ $0_u^+(^1D_2)$ ion-pair states, and molecular constants for the 0_g^+(bb) state are presented.

The potentials of the molecular states discussed in this work are shown in Fig. 1. Various low vibrational levels of the E $0_g^+(^3P_2)$ and f′ $0_g^+(^1D_2)$ ion-pair state are excited *via* the B 0_u^+(ab) valence state using a two-photon optical–optical double resonance (OODR) excitation path. Specific vibrational levels of the D $0_u^+(^3P_2)$ and F′ $0_u^+(^1D_2)$ ion-pair states, respectively, are then populated by ASE transfer from the initially excited levels. Finally, dispersed fluorescence to the 0_g^+(bb) valence state is observed in the near infra-red and

[a] *School of Chemistry, The University of Edinburgh, West Mains Road, Edinburgh, Scotland, UK EH9 3JJ. E-mail: T.Ridley@ed.ac.uk; Fax: +44 (0)1316506453*
[b] *V. A. Fock Institute of Physics, St.Petersburg State University, Ul'janovskaja St.1, Peterhof, 198504, Russia*

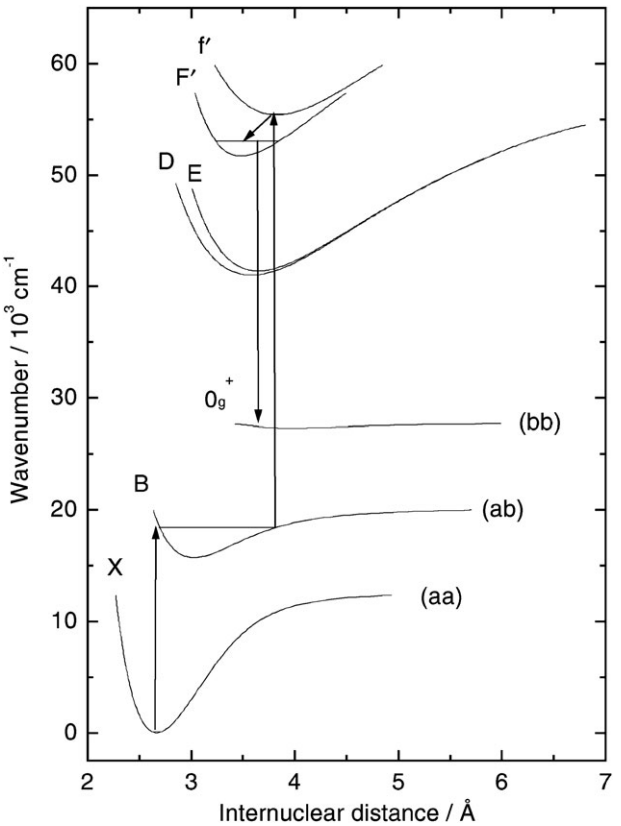

Fig. 1 Potential energy curves of the states of I_2 discussed in this work. The excitation and emission pathways involving the f′ $0_g^+(^1D_2)$ and F′ $0_u^+(^1D_2)$ states are illustrated.

ultra-violet regions, respectively. The pathway involving the f′ $0_g^+(^1D_2)$ and F′ $0_u^+(^1D_2)$ states is illustrated in Fig. 1.

2. Experimental

A XeCl excimer laser (Lambda Physik EMG 201MSC) simultaneously pumped two Lambda Physik dye lasers. An FL 2002 operating with the dye C153 provided the pump photons (~2 mJ per pulse). An FL 3002E operating with fundamental output of Stilbene 3 (≤5 mJ per pulse) and the frequency doubled output of C153 (~1 mJ per pulse), provided the probe photons for excitation of the E $0_g^+(^3P_2)$ and f′ $0_g^+(^1D_2)$ ion-pair states, respectively. The unfocused, counter-propagating pump and probe beams were directed through the glass sample cell that was fitted with Spectrosil quartz windows and contained I_2 at its room temperature vapour pressure (~0.2 Torr). The 90° emission was dispersed by a Jobin Yvon HRS2 (f/7, 0.6 m) monochromator monitored, with one exception, by a Hamamatsu R928 photomultiplier tube whose output was fed into a Stanford Research SR250 gated integrator and stored on a PC. The high resolution F′ $0_u^+(^1D_2)$ → X 0_g^+(aa) emission was detected by a Hamamatsu R955 photomultiplier tube. When recording the D $0_u^+(^3P_2)$ → 0_g^+(bb) and F′ $0_u^+(^1D_2)$ → 0_g^+(bb) emission, any second-order radiation was removed by optical filters. Wavelength calibration of the dispersed fluorescence spectra was achieved by simultaneously recording the emission lines of a neon-filled, lead hollow-cathode lamp.

3. Results

3.1 Emission from the D $0_u^+(^3P_2)$ state

An overview of the emission observed in the range 290–480 nm following excitation of (v = 0, J = 49) of the E $0_g^+(^3P_2)$ state, using an OODR path involving (v = 22) of the B 0_u^+(ab) state, is shown in Fig. 2a. Strong parallel E $0_g^+(^3P_2)$ → B 0_u^+(ab) vibrational bands, with a Gaussian envelope characteristic of emission from (v = 0), are observed between 410 and 435 nm. Weak perpendicular E $0_g^+(^3P_2)$ → A 1_u(aa) and E $0_g^+(^3P_2)$ → C 1_u(aa) emissions are also observed. In addition, strong D $0_u^+(^3P_2)$ → X 0_g^+(aa) emission along with weaker D $0_u^+(^3P_2)$ → a′ 0_g^+(aa) and D $0_u^+(^3P_2)$ → 0_g^+(ab) emissions, all characteristic of (v' = 0), is observed following ASE transfer from the initially excited E $0_g^+(^3P_2)$ state.

The D $0_u^+(^3P_2)$ → 0_g^+(bb) emission observed between 730 and 755 nm using the same excitation path is shown in Fig. 3b. Bound → bound and bound → free structures are observed below and above 748 nm, respectively. A previous study[5] in which very high vibrational levels of the D $0_u^+(^3P_2)$ state were excited by a one-photon path from the X 0_g^+(aa) state also

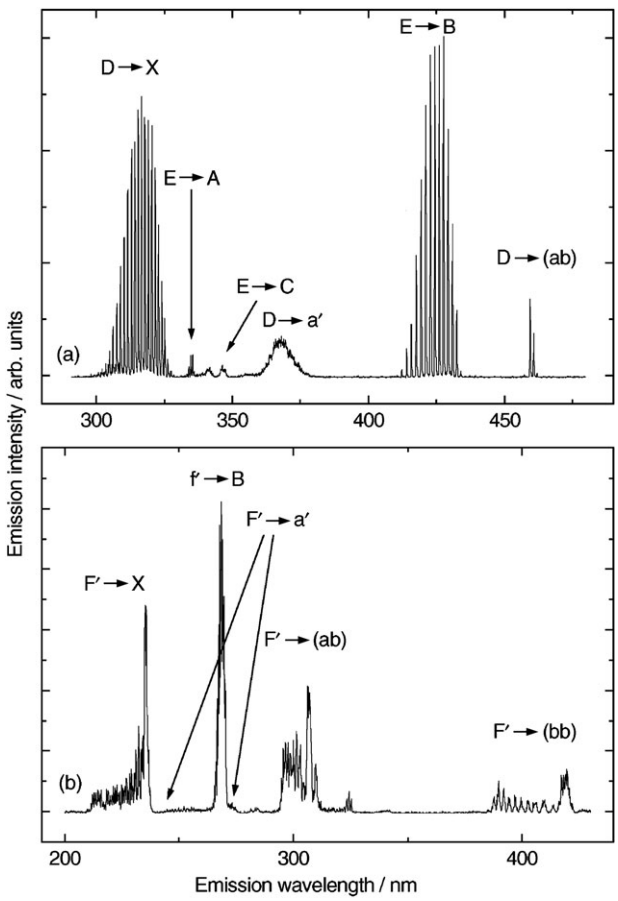

Fig. 2 An overview of the emission observed following excitation of (v = 0) of the E $0_g^+(^3P_2)$ ion-pair state, (a), and the f′ $0_g^+(^1D_2)$ ion-pair state, (b).

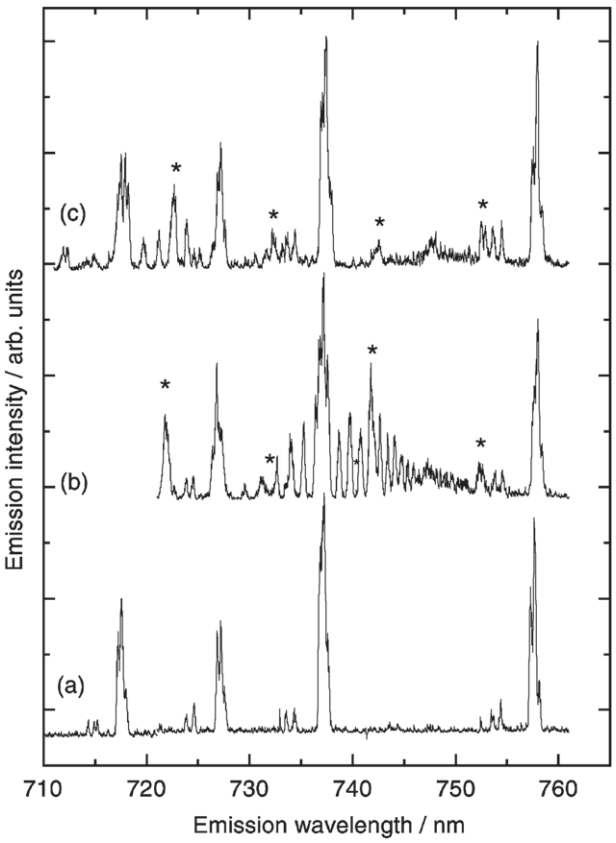

Fig. 3 The D $0_u^+(^3P_2) \rightarrow 0_g^+$(bb) emission spectra following the OODR excitation of ($v = 0$), (b), and ($v = 1$), (c), of the E $0_g^+(^3P_2)$ state. The B 0_u^+(ab) $\rightarrow$ X 0_g^+(aa) emission spectrum observed in the absence of the probe laser is shown in (a). * B 0_u^+(ab) $\rightarrow$ X 0_g^+(aa) emission band observed *via* a cascade process described in the text.

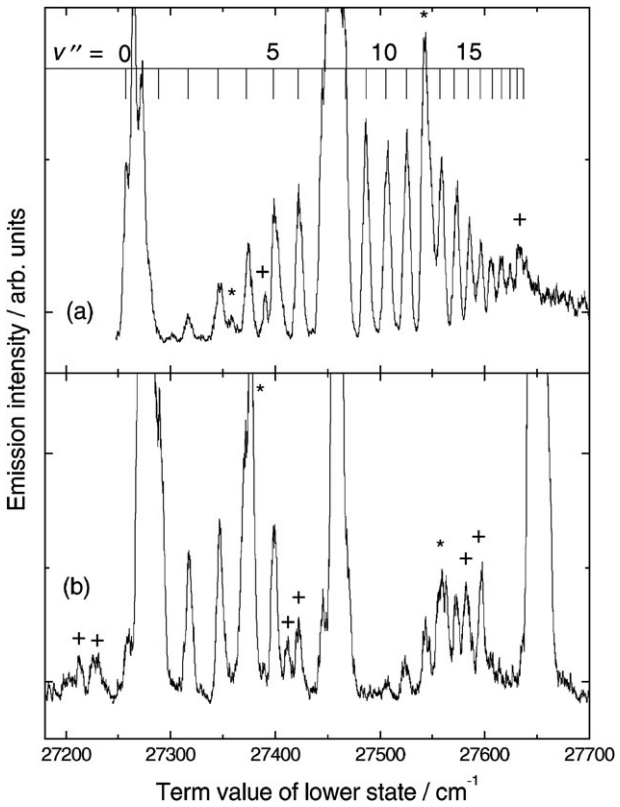

Fig. 4 An expansion of the bound $\rightarrow$ bound region of the D $0_u^+(^3P_2)$ $\rightarrow$ 0_g^+(bb) emission spectra from ($v' = 0$), (a), and ($v' = 2$), (b). + B 0_u^+(ab) $\rightarrow$ X 0_g^+(aa) emission band from the intermediate levels in the OODR excitation path. * B 0_u^+(ab) $\rightarrow$ X 0_g^+(aa) emission band observed *via* a cascade process described in the text.

showed that the D $0_u^+(^3P_2) \rightarrow 0_g^+$(bb) emission has a red extremum around 760 nm.

Unfortunately, part of the B 0_u^+(ab) $\rightarrow$ X 0_g^+(aa) fluorescence from the intermediate level(s) in the OODR scheme also appears in this region as can be seen from the spectrum shown in Fig. 3a which was recorded with the pump laser only. The bands common to both spectra are due to B 0_u^+(ab) $\rightarrow$ X 0_g^+(aa) fluorescence from the intermediate level(s). The same bands also appear in the emission spectrum from ($v = 2$) of the D $0_u^+(^3P_2)$ state, excited *via* ($v = 1$) of the E $0_g^+(^3P_2)$ state, shown in Fig. 3c.

A second class of bands also lie in the region of interest. It was shown previously[2] that very strong E $0_g^+(^3P_2) \rightarrow$ B 0_u^+(ab) ASE also occurs. B 0_u^+(ab) $\rightarrow$ X 0_g^+(aa) fluorescence from the levels populated by this ASE are also observed in a cascade process. Fortunately, only a very small number of levels of the B 0_u^+(ab) state are populated to a detectable degree from a particular E $0_g^+(^3P_2)$ state level. For example, only emission from ($v = 19$ and 20) of the B 0_u^+(ab) state can be detected in this way following excitation of ($v = 0$) of the E $0_g^+(^3P_2)$ state. Bands due to this B 0_u^+(ab) $\rightarrow$ X 0_g^+(aa) cascade fluorescence are indicated by a '*' in Fig. 3b and 3c. These bands appear at different wavelengths in the two spectra as different B 0_u^+(ab) state levels are populated by the E $0_g^+(^3P_2) \rightarrow$ B 0_u^+(ab) ASE.

In spite of the presence of two interfering groups of bands, it is still possible to analyze the D $0_u^+(^3P_2) \rightarrow 0_g^+$(bb) emission, an amplification of which is shown in Fig. 4. The two very intense bands in the emission spectrum from ($v = 0$) of the D $0_u^+(^3P_2)$ state shown in Fig. 4a, together with the weak bands indicated by a '+', are due to B 0_u^+(ab) $\rightarrow$ X 0_g^+(aa) fluorescence from the intermediate level(s). The weak bands indicated by a '*' are due to B 0_u^+(ab) $\rightarrow$ X 0_g^+(aa) cascade fluorescence. The remainder of the spectrum is due to D $0_u^+(^3P_2) \rightarrow 0_g^+$(bb) emission.

The term value (this and all subsequent term values are given relative to ($v = 0$, $J = 0$) of the X 0_g^+(aa) state) of the lower state is shown on the x-axis. The term values are obtained from the term value of the emitting level, calculated from known molecular constants,[6] and the transition wavenumbers measured from the present spectra. For example, the spectrum shown in Fig. 4a was recorded by exciting ($v = 0$, $J = 49$) of the E $0_g^+(^3P_2)$ state (41 404.1 cm^{-1}) from which ($v = 0$, $J = 48$ and 50) (41 015.3 and 41 019.4 cm^{-1}) levels of the D $0_u^+(^3P_2)$ state are populated by ASE. Emission from these two D $0_u^+(^3P_2)$ state levels is then observed to ($J = 47$, 49 and 51) (a span of 7 cm^{-1} using a B value[4] of 0.0172 cm^{-1}) of various vibrational levels of the 0_g^+(bb) valence state. As the four rotational lines in each D $0_u^+(^3P_2) \rightarrow 0_g^+$(bb) band

were not resolved, we use the approximation that the observed bands are centred on the (forbidden) $Q(49)$ rotational transitions, that have an upper-state term value of 41 017.3 cm^{-1}.

The spectrum shown in Fig. 4b was recorded by exciting ($v = 1$, $J = 49$) of the E $0_g^+(^3P_2)$ state. The ($v = 2$, $J = 48$ and 50) levels of the D $0_u^+(^3P_2)$ state are then predominantly populated by ASE, with an upper-state term value for ($J = 49$) of 41 206.6 cm^{-1}. Transitions terminating on two 0_g^+(bb) state levels with lower term values than those in the ($v = 0$) spectrum were observed but these are partially obscured by a strong B 0_u^+(ab) → X 0_g^+(aa) band.

The vibrational numbering in the 0_g^+(bb) valence state cannot be determined from these two spectra. In order to observe a sharp onset for the vibrational progression, *i.e.* at ($v'' = 0$), ($v > 10$) in the D $0_u^+(^3P_2)$ state must be populated. It was not possible to obtain sufficiently good quality D $0_u^+(^3P_2)$ → 0_g^+(bb) emission spectra from these higher levels using this excitation scheme. However, the vibrational numbering of the 0_g^+(bb) state could be determined from emission from the F′ $0_u^+(^1D_2)$ third tier ion-pair state, populated by ASE from the f′ $0_g^+(^1D_2)$ ion-pair state, as described below.

3.2 Emission from the F′ $0_u^+(^1D_2)$ state.

The rovibronic levels ($v = 0$ and 1, $J = 49$) of the f′ $0_g^+(^1D_2)$ state were excited using an OODR path involving ($v = 25$) of the B 0_u^+(ab) state. An overview of the emission observed following excitation of ($v = 0$) of the f′ $0_g^+(^1D_2)$ state is shown in Fig. 2b. A Gaussian envelope of f′ $0_g^+(^1D_2)$ → B 0_u^+(ab) vibrational bands, characteristic of emission from ($v = 0$), are observed around 270 nm (these are not resolved in the spectrum in Fig. 2b).

Strong F′ $0_u^+(^1D_2)$ state emission is also observed following ASE transfer from the initially excited f′ $0_g^+(^1D_2)$ state. Each F′ $0_u^+(^1D_2)$ emission system appears over a wide wavelength range clearly indicating that they emanate from vibrational levels with ($v > 0$). It was shown previously[2] that ASE transfer occurs to the vibrational levels of the lower state that have the largest FC overlaps with the initially-populated level. In the case of the E $0_g^+(^3P_2)$/D $0_u^+(^3P_2)$ and γ $1_u(^3P_2)$/β $1_g(^3P_2)$ pairs of ion-pair states, the ASE transfer involves a very small change in v, since their internuclear separations are very similar. However, the f′ $0_g^+(^1D_2)$ and F′ $0_u^+(^1D_2)$ states have, respectively, the largest and smallest internuclear separations of the characterized ion-pair states of I_2.[9,10] Consequently, ($v = 0$) of the f′ $0_g^+(^1D_2)$ state has the largest FC overlaps with ($v = 8$–11) of the F′ $0_u^+(^1D_2)$ state as shown in Table 1.

The numbering of the F′ $0_u^+(^1D_2)$ state vibrational levels accessed by ASE can be confirmed from an analysis of the F′ $0_u^+(^1D_2)$ → X 0_g^+(aa) emission as the lower state molecular constants are known.[11] An expansion of the highest transition wavenumber region of the F′ $0_u^+(^1D_2)$ → X 0_g^+(aa) emission following ASE transfer from ($v = 0$) of the f′ $0_g^+(^1D_2)$ state is shown in Fig. 5. The ladders indicate the position of the $Q(49)$ lines (see above) of the vibrational transitions calculated from the molecular constants.[10,11] The strongest bands originate in ($v' = 9$ and 10) with weaker contributions from ($v' = 8$ and 11), in line with the magnitudes of the FC overlaps shown in Table 1. The band with the largest transition wavenumber in each ladder corresponds to a transition to ($v = 30$) of the X 0_g^+(aa) state. Each ladder also shows the calculated FC factors for the transitions from a particular upper state level. The relative intensities of the ladders are adjusted to match the experimental spectrum. It can be seen that the calculated positions and the intensities are in reasonable agreement with the experimental data and hence the upper state vibrational assignments are confirmed.

Table 1 Franck–Condon factors[7,8] of the rotationless laser-excited v-levels of the f′ $0_g^+(^1D_2)$ state with selected v-levels of the F′ $0_u^+(^1D_2)$ state

	$v_{f'}$	
$v_{F'}$	0	1
5	0.03	0.08
6	0.06	0.11
7	0.10	0.11
8	0.14	0.06
9	0.16	0.01
10	0.16	0.01
11	0.13	0.04
12	0.10	0.09
13	0.06	0.12
14	0.03	0.12
15	0.02	0.10

It can be seen from the spectrum in Fig. 2b that the F′ $0_u^+(^1D_2)$ → 0_g^+(bb) now lies in a wavelength region where there are no other emission systems. The ten minima in the spectrum show that ($v' \sim 10$) provided that the spectrum is of the reflection type. A high-resolution scan of the low-wavelength region of the system is shown in Fig. 6a. As was the case with the D $0_u^+(^3P_2)$ → 0_g^+(bb) emission, fully resolved vibrational structure can be observed and is assigned to transitions from ($v = 8$–11) of the F′ $0_u^+(^1D_2)$ state to low-v levels of the 0_g^+(bb) state. The band with the largest

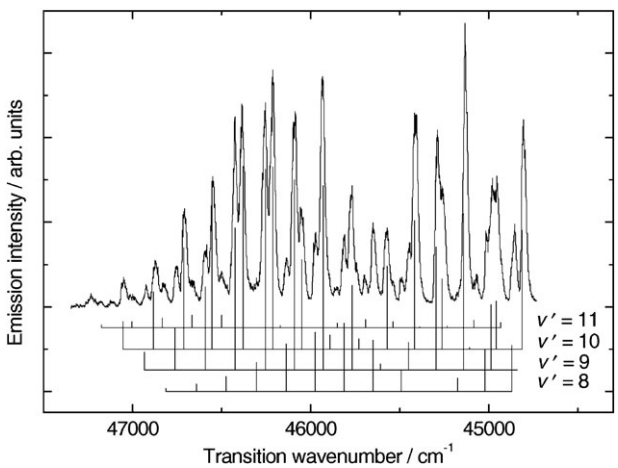

Fig. 5 An expansion of part of the F′ $0_u^+(^1D_2)$ → X 0_g^+(aa) emission, ($v' = 8$–11), following ASE transfer from ($v = 0$) of the f′ $0_g^+(^1D_2)$ state. The band with the largest transition wavenumber in each ladder corresponds to a transition to ($v = 30$) of the X 0_g^+(aa) state.

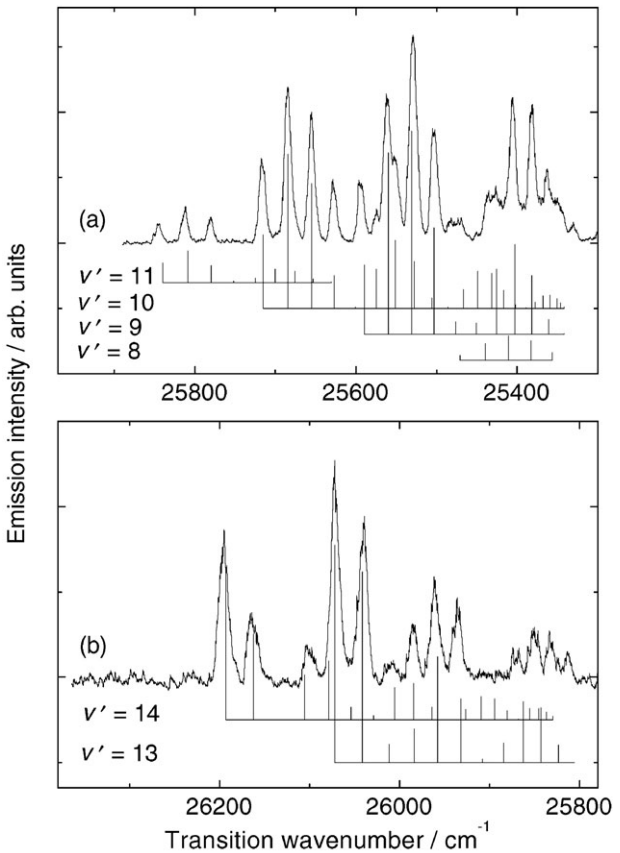

Fig. 6 An expansion of part of the F′ $0_u^+(^1D_2) \rightarrow 0_g^+$(bb) emission following excitation of ($v = 0$), (a), and ($v = 1$), (b), of the f′ $0_g^+(^1D_2)$ state. The band with the largest transition wavenumber in each ladder corresponds to a transition to ($v = 0$) of the 0_g^+(bb) state.

transition wavenumber in each ladder corresponds to a transition to ($v = 0$) of the 0_g^+(bb) state.

This numbering of the 0_g^+(bb) state vibrational levels is confirmed from the emission observed following excitation of ($v = 1$) of the f′ $0_g^+(^1D_2)$ state shown in Fig. 6b. The magnitude of the FC overlaps dictate that ASE transfer occurs predominantly to ($v' = 13$ and 14) of the F′ $0_u^+(^1D_2)$ state (see Table 1). The transitions in each of the two vibrational progressions with the largest transition wavenumber in Fig. 6b are now the most intense and are assigned as those with ($v'' = 0$).

3.3 Determination of molecular constants

The 0_g^+(bb) state was modelled by a modified Morse potential as described previously,[3] and the F′ $0_u^+(^1D_2)$ state was defined by its RKR turning points.[10] The lower state potential was then shifted to larger or smaller R and the FC factors calculated. A constant transition dipole function was used since only the relative intensities of the first two or three vibrational bands, even in favourable cases, were free from overlap with neighbouring progressions.

The best simulations of the observed intensities, as judged by the match of the ($v'' = 0$–3) bands from all six upper state levels, are shown as ladders in Fig. 6. The largest transition wavenumber band in each progression is due to a transition to ($v'' = 0$). The simulations were obtained using a slightly larger R_e value for the 0_g^+(bb) state than that calculated[4] (3.952 ± 0.005 Å, compared with 3.928 Å). The relative intensities of the ladders are adjusted to match the experimental spectrum.

The term values, G_v, for ($J = 49$) of ($v = 0$–2) of the 0_g^+(bb) state obtained from the F′ $0_u^+(^1D_2)$ emission are combined with those for ($v = 3$–19) obtained from the D $0_u^+(^3P_2)$ emission and presented in Table 2. The term values were fitted to a second-order polynomial of the form

$$G_v = a + b(v + 1/2) - c(v + 1/2)^2 \qquad (3)$$

in which b and c equal ω_e and $\omega_e x_e$ for ($J = 0$), to produce the coefficients: $a = 27\,245.9 \pm 0.7$ cm^{-1}, $b = 31.2 \pm 0.2$ cm^{-1} and $c = 0.61 \pm 0.01$ cm^{-1}. The real error associated with a, which is limited by the accuracy of the calibration procedure, is greater than that generated from the statistical fit of the data and is estimated to be ±2 cm^{-1}.

The calculated a coefficient is derived from transitions terminating on ($J = 49$). Using a rotational constant $B_e = 0.01701$ cm^{-1}, resulting from the value for R_e of 3.952 Å obtained from the simulation of the observed intensities, gives 41.7 cm^{-1} of rotational energy in ($J = 49$). Thus, the true T_e

Table 2 Observed, G_v(obs.), and calculated, G_v(calc.), term values, relative to ($v = 0$, $J = 0$) of the X 0_g^+(aa) state, of ($J = 49$) of the vibrational levels of the 0_g^+(bb) state. The calculated values were obtained from second-order polynomials with the constants given in the text

v	G_v(obs.)/cm^{-1}	G_v(obs.) − G_v(calc.)/cm^{-1}
0	27 261.0	0.0
1	27 292.0	1.0
2	27 320.5	0.7
3	27 346.6	−0.7
4	27 373.1	−0.4
5	27 398.5	−0.2
6	27 422.6	0.9
7	—	—
8	—	—
9	27 485.5	−1.9
10	27 505.6	−0.9
11	27 524.7	0.3
12	27 541.8	0.7
13	27 557.7	1.1
14	27 572.9	2.1
15	27 584.7	0.8
16	27 595.6	−0.1
17	27 605.7	−0.7
18	27 615.1	−0.3
19	27 623.1	−0.9

Table 3 Molecular constants of the 0_g^+(bb) valence state of I_2

	Present work	Literature[4]
T_e/cm^{-1}	27 311.3 ± 2	—
D_e/cm^{-1}	442.0 ± 2	435
ω_e/cm^{-1}	31.9 ± 0.2	33.8
B_e/cm^{-1}	0.01701 ± 0.00004	0.0172
R_e/Å	3.952 ± 0.005	3.928

(27 245.9 – 41.7 + 107.1 cm^{-1}) and D_e values must be 27 311.3 ± 2 and 442.0 ± 2 cm^{-1}, respectively. The b constant, corrected for the J-dependency, gives ω_e as 31.9 cm^{-1}. The molecular constants of the 0_g^+(bb) state are summarized in Table 3.

4. Conclusions

A sufficient range of vibrational levels of the D $0_u^+(^3P_2)$ and, in particular, the F′ $0_u^+(^1D_2)$ ion-pair states can be populated by ASE from the readily accessible E $0_g^+(^3P_2)$ and f′ $0_g^+(^1D_2)$ ($v = 0$) states to establish the numbering of the vibrational progressions for the transitions D $0_u^+(^3P_2)$, F′ $0_u^+(^1D_2)$ (v') → 0_g^+(bb) (v'') seen in fluorescence. Although the rotational branch splitting in the lower shallow-bound state could not be resolved, R_e can be sufficiently well located to ±0.005 Å for T_e and D_e values to be calculated from the vibrational term values obtained for a single J state.

Acknowledgements

VA acknowledges financial support from an International Exchange Programme grant from The Royal Society of Edinburgh.

References

1 L. Allen and G. I. Peters, *Phys. Rev. A*, 1973, **8**, 2031.
2 V. A. Alekseev, T. Ridley, K. P. Lawley and R. J. Donovan, *Chem. Phys. Lett.*, 2007, **443**, 34.
3 T. Ridley, K. P. Lawley and R. J. Donovan, *J. Chem. Phys.*, in press.
4 W. A. de Jong, L. Visscher and W. C. Nieuwpoort, *J. Chem. Phys.*, 1997, **107**, 9046.
5 R. J. Exton and R. J. Bella, *J. Quant. Spectrosc. Radiat. Transfer*, 2004, **86**, 267.
6 J. Tellinghuisen, *J. Mol. Spectrosc.*, 2003, **217**, 212.
7 R. J. LeRoy, Chemical Physics Research Report No. CP-425, University of Waterloo, 1992.
8 R. J. Le Roy, Chemical Physics Research Report No. CP-655, University of Waterloo, 2002.
9 T. Ishiwata, J. Yamada and K. Obi, *J. Mol. Spectrosc.*, 1993, **158**, 237.
10 T. Ishiwata, A. Tokunaga, T. Shinzawa and I. Tanaka, *J. Mol. Spectrosc.*, 1986, **117**, 89.
11 P. Luc, *J. Mol. Spectrosc.*, 1980, **80**, 41.

